



ELSEVIER

Tectonophysics 308 (1999) 119–131

TECTONOPHYSICS

www.elsevier.com/locate/tecto

Recent geodynamic characteristics in the Arabian–Eurasian and Indian–Eurasian collision region by active fault data

V.G. Trifonov^{a,*}, G.A. Vostrikov^a, R.V. Trifonov^a, A.S. Karakhanian^b, O.V. Soboleva^a

^a Geological Institute of the Russian Academy of Sciences, 7 Pyshevsky, Moscow, 109017, Russia

^b Institute of Geological Sciences of the National Academy of Sciences, 24a Bagramian Ave, Yerevan, 375019, Armenia

Received 27 March 1998; accepted 22 October 1998

Abstract

A part of the Alpine–Himalayan orogenic belt is studied, limited by 30–104°E and by 26–46°N to the west of 64°E and 26–56°N to the east of 64°E. A technique is proposed to calculate the field of the recent (Late Pleistocene and Holocene) deformation rate tensors in the upper crust (15 to 20 km) by active fault data. A hydrodynamic model of the medium is used for the calculation. Monotonous fault segments as long as 10–15 km are taken as the elementary cells of the medium. The cell square (the length multiplied by the depth) multiplied by the displacement vector magnitude, gives the geometric moment. Similar components of the local tensors of the geometric moments are summarized within the windows into which the region is divided. Finally, parameters of the axes of principal rates of deformation are calculated, and their directions and magnitudes are mapped. This tectonic deformation is compared with the seismotectonic one calculated by focal mechanisms of earthquakes. The compiled maps show: a concentration of high deformation rates in the plate boundary zones (especially in front of the southern plate syntaxes) and a smaller concentration in some microplate boundary zones; a predominance of the N–S-trending shortening and of strike-slip type of deformation. The rates of shortening and lengthening are usually almost equal to each other and differ essentially (the shortening rate is higher than the lengthening) only in specific sites. These are areas of intense recent detachment or late Quaternary volcanism. It seems that the double-axis lengthening (extension) is suitable for these processes. © 1999 Elsevier Science B.V. All rights reserved.

Keywords: active tectonics; recent geodynamics; tensor of tectonic deformation rates

1. Introduction

The tectonically complicated region under discussion occupies the areas of recent collision of the Arabian and Indian plates and the Eurasian plate. It is limited by 30–104°E and by 26–46°N to the west of 64°E and 26–56°N to the east of 64°E. This seismic region contains many active faults and other active

structures that can be related to the high recent seismicity (Fig. 1). It is difficult sometimes to identify some particular seismic events with the activity on individual faults or fault zones and to understand the tectonic features of the seismic source. In this situation it seems useful for seismic hazard assessment to find some general characteristics of recent tectonic activity that would give a possibility to compare different parts of the region. These characteristics are the components of the tensor of recent deformation rates.

* Corresponding author. E-mail: trifonov@ginran.msk.su

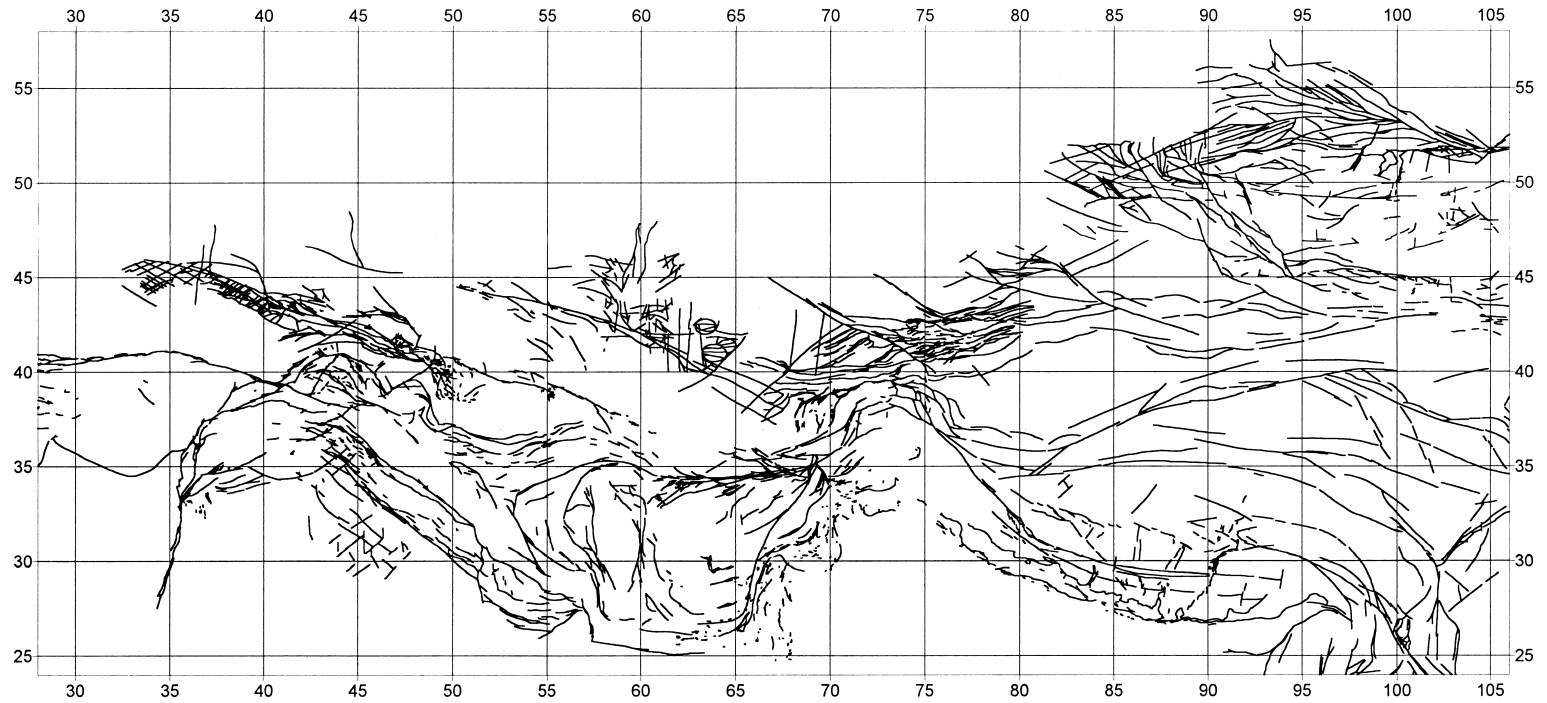


Fig. 1. Active faults of the Arabian–Eurasian and Indian–Eurasian collision regions.

2. Source data

Primary data for calculating the recent deformation field are obtained from a data set including the parameters of active faults, namely faults with offsets or other manifestations of displacements during the last 100,000 years (Trifonov, 1985, 1996). We compiled a database of necessary parameters of every fault used for the calculation. These are: (1) fault number and name; (2) source of the information; (3) geographic coordinates of the fault points, adequate to reproduce the fault line of a scale of 1 : 1,000,000; (4) direction of the fault dip; (5) angles of the dip (minimum 'min', most probable 'mp', and maximum 'max'); (6) sense of the lateral component of motion (if present), dextral or sinistral; (7) presence of an extension component; (8) sense of the vertical component of motion (if present), thrust-reverse or normal; (9) average rates of lateral motion, mm/year (min, mp, and max); (10) average rates of extension, mm/year (min, mp, and max); (11) average rates of vertical motion (min, mp, and max).

The majority of the necessary parameters (1, 2, 3, 4, 6, 7, and 8) were selected from the database of active faults collected during Project II-2, 'World Map of Major Active Faults', of the International Lithosphere Program (Trifonov and Machette, 1993; Ioffe et al., 1993; Trifonov, 1996, 1997; Ioffe and Kozhurin, 1996). The papers and special contributions of K.E. Abdrakhmatov, N.N. Ambraseys, A.A. Barka, M. Berberian, Ding Guoyu, K. Hessami, A.S. Karakhanian, S.I. Kuloshvili, N.V. Lukina, P. Molnar, T. Nakata, A.A. Nikonov, F. Saroglu, V.P. Solonenko, P. Tapponier, V.G. Trifonov, as well as K. Allen, V.S. Burtman, O. Emre, Deng Qidong, T.P. Ivanova, S.D. Khilko, M.L. Kopp, A.I. Kozhurin, I. Kuscu, K.G. Levi, V.I. Makarov, E.E. Milanovsky, S.I. Sherman, A. Sinha, A.V. Timush, R.S. Yeats, and others were used for compiling the database for the region under discussion. We used the same database also for the detection of dip angles and rates of motion on the faults. The rates could be the result of creep or the sum of seismic pulses and were determined mostly by geological and geomorphological data. If these data were not present for a fault, we estimated the parameters hypothetically in a wide interval of possible values by using neotectonic (pre-late Quaternary) and seismological (focal

mechanisms, geometry of epicentral areas, seismic moments, and so on) data, or a similarity of features of the fault as compared with other faults. We preferred not to use geodetic determinations not supported by geological and/or geomorphological evidence, because sometimes they give essentially higher values of the rates. Differences between min- and max-values show the accuracy and reliability of the estimations. If any of parameters 4–11 varied along the fault, the latter was subdivided into monotonous segments.

The unpublished 'Catalog of Focal Mechanisms of Earthquakes' by O.I. Gushchenko, A.A. Maystryukov and V.N. Petrov kindly made available by the authors, was used for calculating the components of the tensor of the seismotectonic deformation in the region. The earthquake magnitudes were checked and corrected by using the 'New, 1996 Catalog of Earthquakes in Northern Eurasia from Ancient Times up to 1992', compiled by the Institute of Physics of the Earth of the Russian Academy of Sciences, and edited by N.V. Kondorskaya and V.I. Ulomov (manuscript). The Catalog of Focal Mechanisms contains more than 900 events in the region under discussion. The focal parameters of some earthquakes were corrected by the results of O.V. Soboleva's determinations of Central Asian earthquakes (33 events) and by the new determinations by L.M. Balakina of the strongest earthquakes in the region.

3. Computational method and results

The methods of calculation were described before (Trifonov et al., 1997) and hence they will be discussed here only briefly. A hydrodynamic model of the upper crust (about 15 km thick) is proposed, implying that discrete displacements on individual active faults are represented formally as elements of a unified process of viscous flow in a large volume of a medium. One of the macroscopic parameters of the flows is the tensor of deformation rates. It can be calculated as an average effective parameter for the large spatial-temporal volumes of a medium (windows). The temporal condition is completely fulfilled, because the duration of the Late Pleistocene and Holocene (about 100,000 years) is much

larger than the recurrence interval of the strongest earthquakes in the region. For the fulfilment of the spatial conditions, the lateral dimensions of the volume (space window) must on average be longer than the largest fault. On the other hand, they must not so large as to lose variations of the characteristics of deformation. The whole region was divided into windows, their sides being along parallels and meridians, in two ways: $1^\circ \times 1.25^\circ$ in size without overlapping, and $3^\circ \times 3.75^\circ$ in size with overlapping, with steps of 1° and 1.25° , respectively. The first discretization, giving a more detailed picture, was used for the calculation of the directions of the principal deformation. The second discretization, with a more pronounced smoothing effect, was used for calculation of both the directions and magnitudes of the principal deformation. The monotonous fault segments were also subdivided into elementary cells, from 10 to 20 km long, with constant strikes and dips.

The cell thickness L_3 (the fault penetration depth that cannot exceed 15 km) was calculated by using its correlation with the fault length L_1 , if L_1 was not more than 50 km (Sidorenko, 1978). We introduce the value of a 'geometric moment' M that is the full vector of the rate of motion along the area of the cell S , multiplied by L_1 and multiplied by L_3 . M is a tensor. For each cell we calculated its components of the geographic coordinate system (east, north, and zenith). All similar components of the tensor were summarized and normalized to a unit of the window volume and time:

$$\dot{\epsilon}_{lm} = \frac{1}{2} \frac{\sum_n M_{lm}^n}{\Delta V} \quad (1)$$

where n is number of the cells within a window, and ΔV is an area of the window multiplied by the thickness of the active layer (15 km). After Kostrov (1975), the left side of the equation is an average tensor of deformation rate at the expense of motion along active faults. Further, we calculated the principal rates of deformation (M_1 , M_2 and M_3) using the well-known approach of rock mechanics (Jaeger and Cook, 1969), and attributed them to the centres of windows. The resulting tensor field is shown by the directions of the principal rates of deformation (shortening, lengthening, intermediate) and by isolines of their magnitudes (Figs. 2–4). The results of the calculations for the mp values of

parameters 5 and 9–11 are represented in Figs. 2–4. Calculations for the min- and max-values did not show essential differences in principal rate directions and gave only smaller or larger values of these magnitudes.

The components of the tensor of the seismotectonic deformation are calculated in an analogous way. Here M is the seismic moment of the individual earthquake and it is calculated by using its correlation with the earthquake magnitude. The focal mechanism gives an orientation of the M tensor. The tensor of the seismotectonic deformation is calculated as the sum of the tensors of the individual earthquakes occurring within some volume (window) V during the time interval of 100,000 years (Eq. 1). The technique is described in detail in papers of Riznichenko (1977) and Soboleva (1988). We used the same overlapping windows $3^\circ \times 3.75^\circ$ for a calculation of the seismotectonic deformation, as was done for the tectonic one. The directions of the principal axes of the seismotectonic deformation and the values of the Lade–Nadai coefficient are presented in Figs. 5 and 6.

4. Discussion

The axes of principal shortening M_3 (Fig. 2) are subhorizontal almost all over the region and trend mostly north–south. This supports the idea that the main source of the recent deformation in the region is the motion and pressure of the Arabian and Indian plates. Deviations are characteristic of the areas west and east of the Pendjab and Arabian syntaxes and near the northeastern flank of the Indian plate, and are most significant in the eastern part of Tibet and its eastern boundary zone, in Yunnan, the eastern Sayans, Quetta, northern Anatolia and the northern Aral region. These deviations depend on strain re-orientation in the flanks of the southern plates and peculiarities of its transformation in local zones. In the rare cases of a local extension M_3 is almost vertical. It is found in some sites of Tibet, near the Hubsugul Lake in northern Mongolia, the eastern Aral and the Lut region and in the northern slope of the northern Caucasus foredeep.

The axes of principal lengthening, M_1 (Fig. 3), often trend east–west and deviate from this general

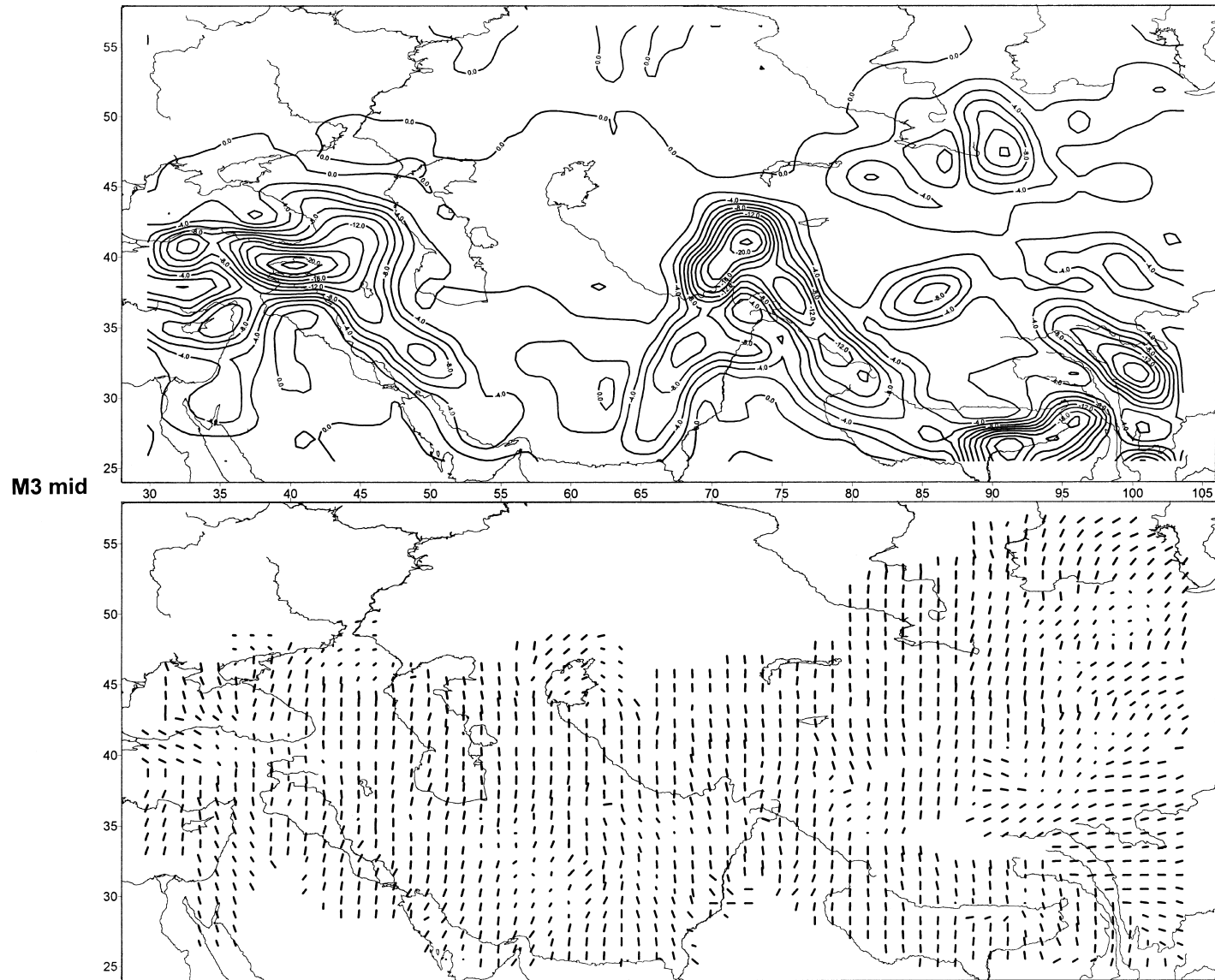


Fig. 2. Recent tectonic deformation in the region by active fault data: magnitudes of rates ($M_3 \times 10^9$) and orientation of principal shortening, calculated for the most probable values of parameters and for the windows of $3^\circ \times 3.75^\circ$; length of the M_3 axes is proportional to their angle with respect to the vertical.

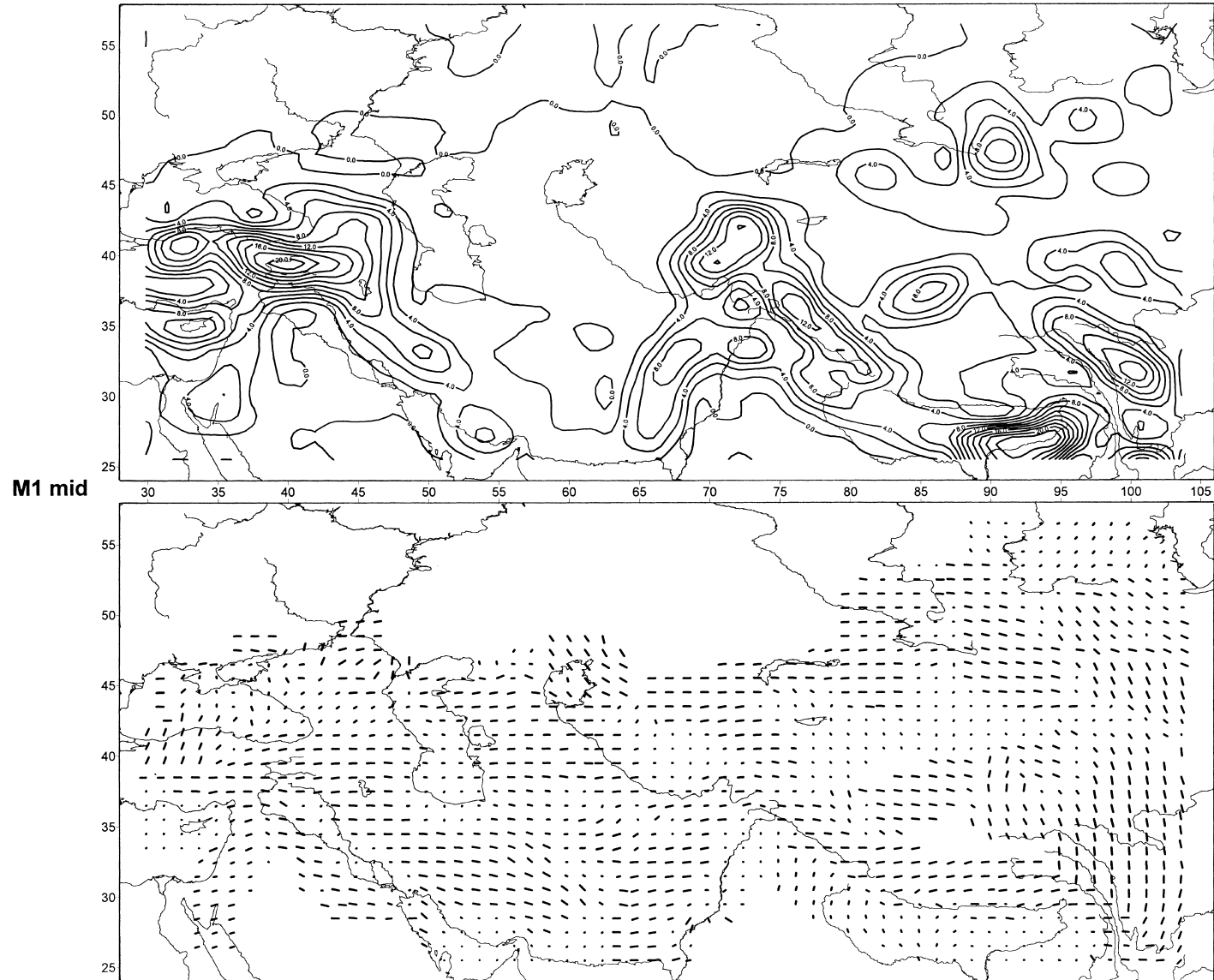


Fig. 3. Recent tectonic deformation in the region by active fault data: magnitudes of rates ($M_1 \times 10^9$) and orientation of principal lengthening, calculated for the most probable values of parameters and for the windows of $3^\circ \times 3.75^\circ$; length of the M_1 axes is proportional to their angle with respect to the vertical.

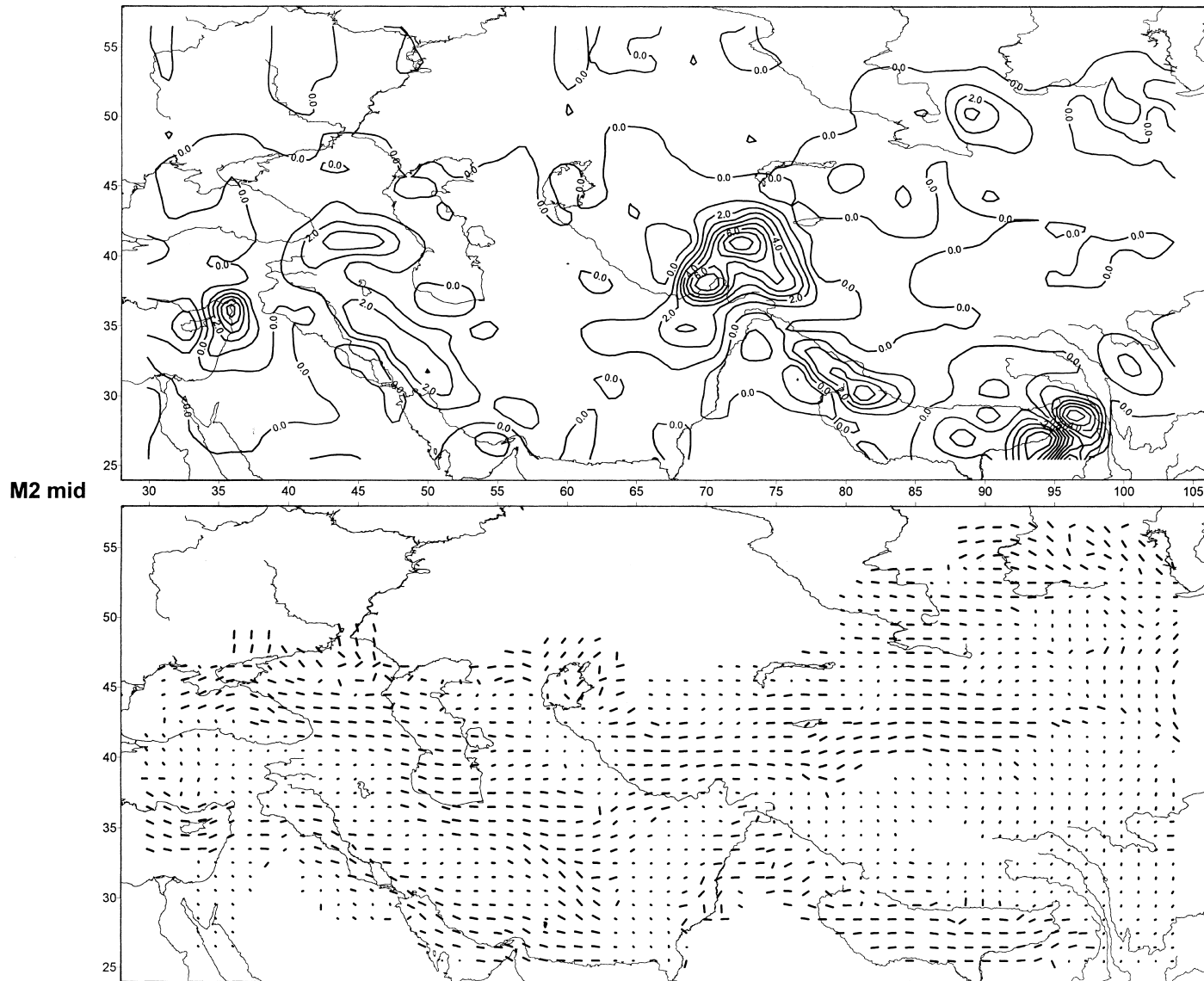


Fig. 4. Recent tectonic deformation in the region by active fault data: magnitudes of rates ($M_2 \times 10^9$) and orientation of principal intermediate deformation calculated for the most probable values of parameters and for the windows of $3^\circ \times 3.75^\circ$; length of the M_2 axes is proportional to their angle with respect to the vertical.

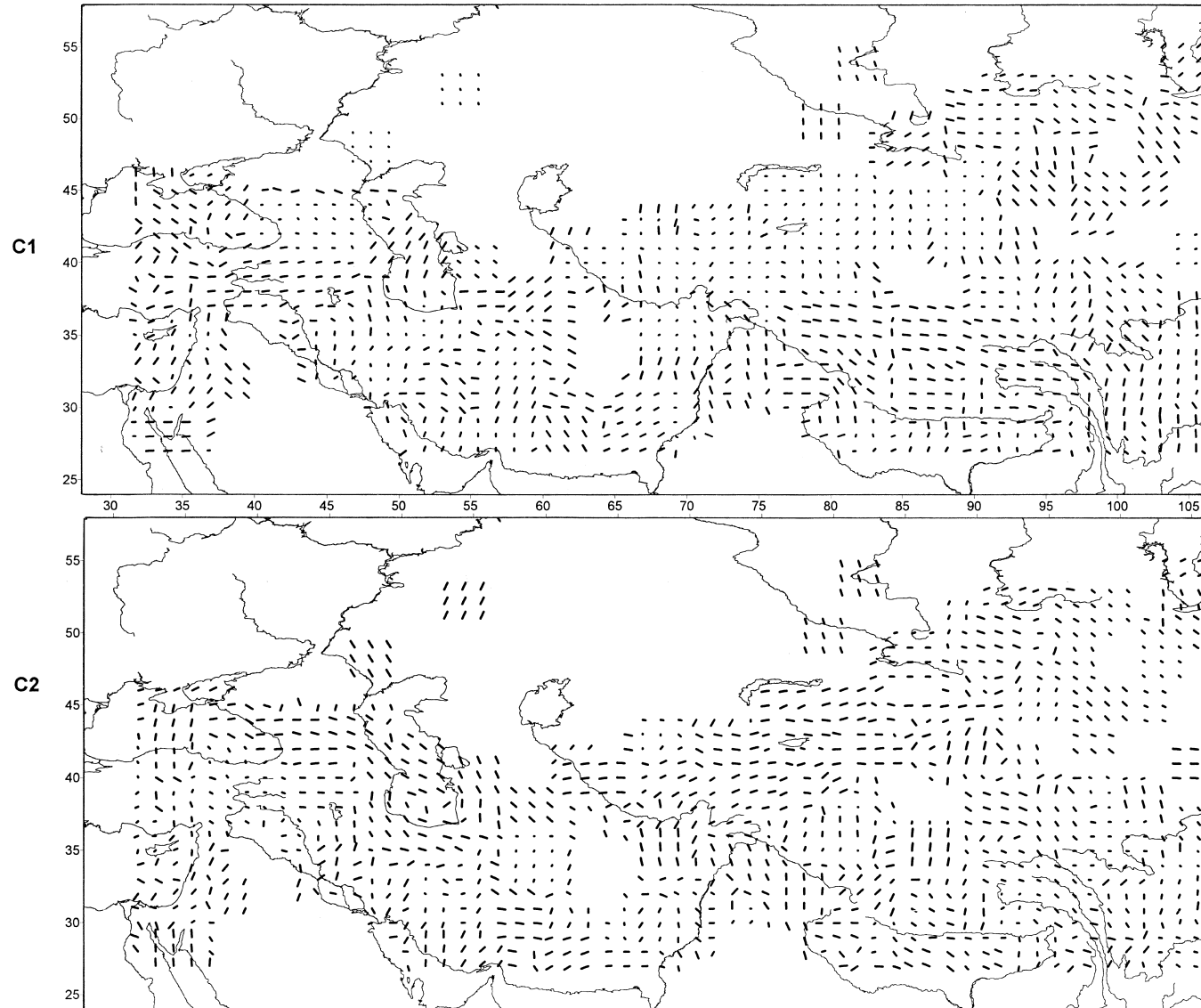


Fig. 5. Seismotectonic deformation in the region from data of focal mechanisms of earthquakes: orientation of principal lengthening C_1 and principal intermediate deformation C_2 calculated for the windows of $3^\circ \times 3.75^\circ$; lengths of the C_1 and C_2 axes are proportional to their angle with respect to the vertical.

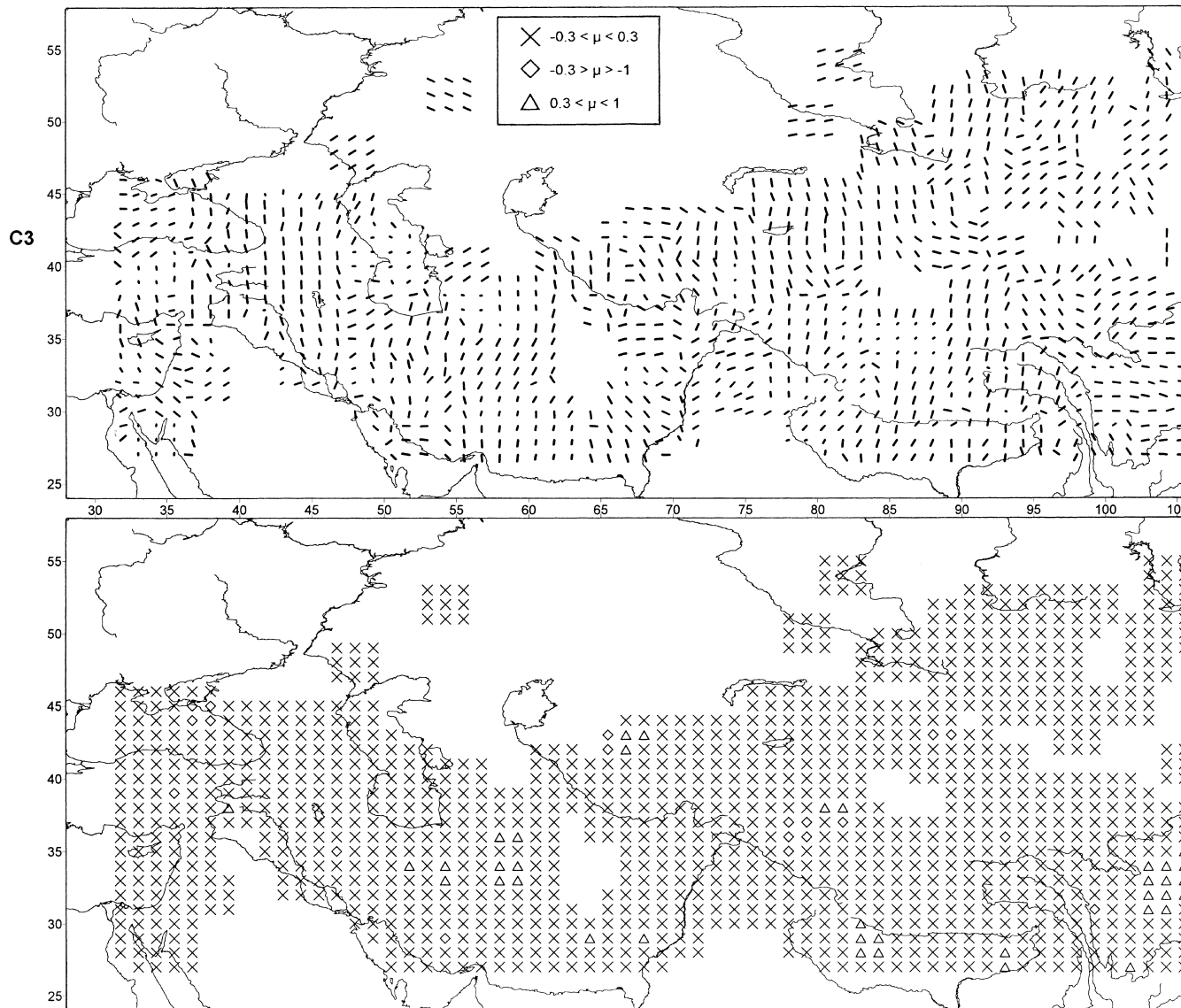
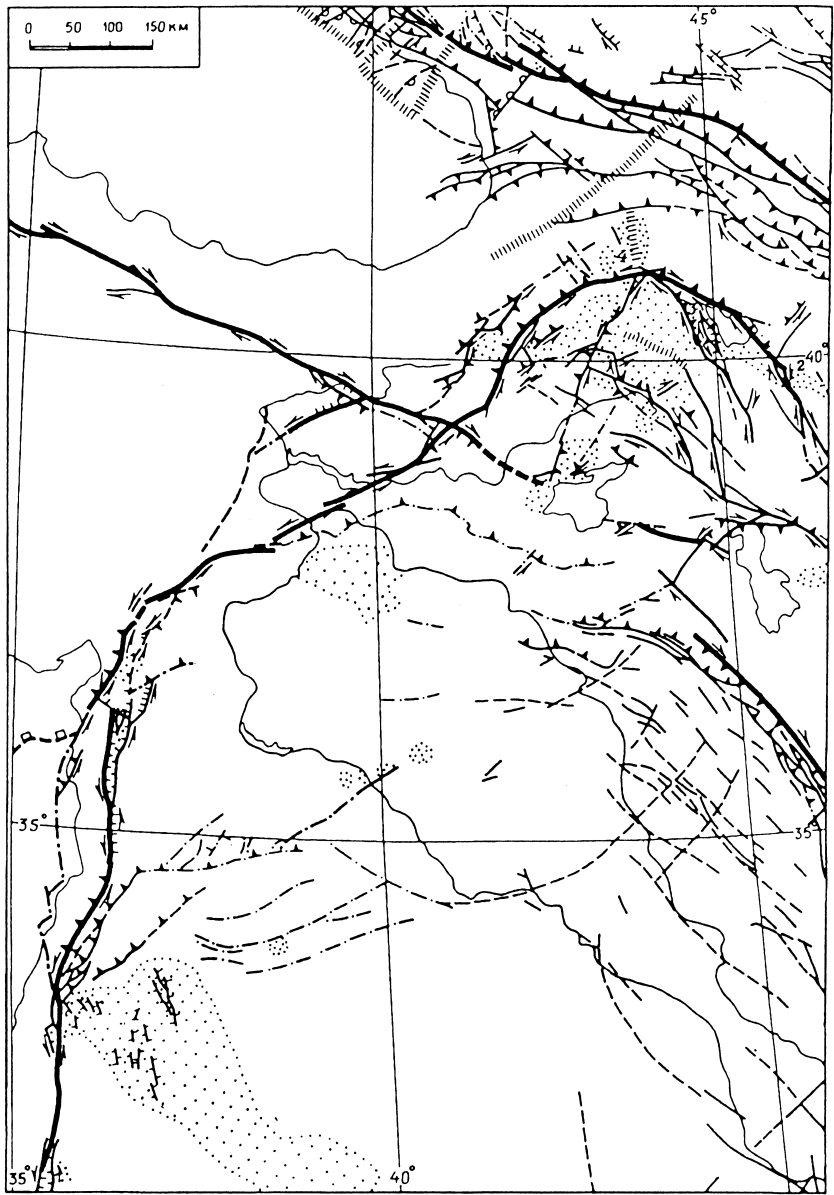
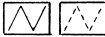
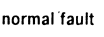
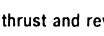
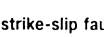
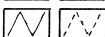
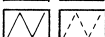
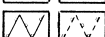


Fig. 6. Seismotectonic deformation in the region from data of focal mechanisms of earthquakes: orientation of principal shortening C_3 and values of the Lade-Nadai coefficient calculated for the windows of $3^\circ \times 3.75^\circ$; length of the C_3 axes is proportional to their angle with respect to the vertical. Values of the Lade-Nadai coefficient: $\times = -0.3 \leq \mu \leq 0.3$; $\diamond = -0.3 > \mu > -1$; $\Delta = 0.3 < \mu < 1$.



-   normal fault
-   thrust and reverse fault
-   extension fault
-   strike-slip fault
-   flexure
-   unknown
-   seismic focal zone
-   deep-seated fault zone

Age of last manifestations of activity

-  Middle Pleistocene
-  Late Pleistocene and Holocene, including historical and contemporary

Rate of motion

-  $V \geq 5 \text{ mm/a}$
-  $1 \leq V < 5 \text{ mm/a}$
-  $V < 1 \text{ mm/a}$

direction in areas with deviations of M_3 . The M_1 axes are subhorizontal in 60–70% of the territory. The subhorizontal orientation of both M_3 and M_1 axes testifies to the predominance of strike-slip tectonics in the whole region. However, the M_1 axes are subvertical more often than the M_3 axes. This is characteristic for areas of intensive young thrusting and folding: the Himalayas, the western and eastern Tien Shan and the major part of Sayans, Baluchistan, Makran, Alborz, the Cyprus arc and partly the Great Caucasus. It is interesting to see that the same situation is found in the weakly deformed Tarim basin.

High values of the M_3 and M_1 rates are characteristic for wide zones around the Arabian and Indian plates as well as at the eastern flank of Tibet and northern Anatolia; the highest values are observed in the northern fronts of the southern plates. High deformation rates are also found in the Red River region, the northwestern and northeastern flanks of Qaidam, the Mongolian Altai, the junction of the Cyprus arc and the Levant fault zone and in the central part of the Great Caucasus. Thus, recent deformation is concentrated along the boundaries of the main plates and the most active smaller Anatolian and Tibetan plates, as well as at the boundary of the Dzungarian and Mongolian microplates. These areas are zones of high seismicity, but a straight correlation between the crustal seismic activity and the rates of deformation has not been found.

By taking into account the min- and max-values, total transverse shortening of the upper crust of the Alpine–Himalayan collision belt was found to be equal to 3 ± 1 cm/year in the Tien Shan–Pamir–Himalayan segment and 2 ± 1 cm/year in the Caucasus–Arabian segment.

Fig. 4 shows that the M_2 rates are very low, i.e. the M_3 and M_1 rates are almost equal in most of the region. This indicates a double-axis type of deformation corresponding, in terms of rock mechanics, to a pure shear deformation. However, in some areas the difference between the magnitudes of shortening and lengthening becomes noticeable. The only area where the M_3 rates are essentially less than the M_1

rates (the M_2 rates are negative) is the Yunnan region in front of the Assam syntaxis. This may be related to the sharply variable deformation field of the region. In the remaining areas the M_3 rates exceed the M_1 rates. The highest differences are found in front of the Pendjab syntaxis (Pamir, central Tien Shan and the Tadjik basin) and in the frontal part of the Assam syntaxis of the Indian plate. The differences are high enough in the Himalayas, near the Teletskoe Lake graben (Altai) in the northwestern termination of the Kobdo dextral active fault zone, in the northeastern part of the main recent fault of Zagros, in the northern part of the Levant fault zone, and near the North Armenian arc with active faults. Larger values of the M_3 with respect to M_1 rates means that a double-axis lengthening takes place there. These areas in the Himalayas and in front of the Indian plate are zones of intense recent detachment. Zagros was characterized by a Pliocene and earlier Quaternary volcanism. The latter continued till the late Quaternary in the Levant and northern Armenian (Fig. 7). So, the double-axis lengthening seems to be a suitable geodynamic situation for both detachment tectonics and volcanism in the collision belt.

Areas of Late Pleistocene and Holocene volcanism form the NNE–SSW-trending interrupted transverse belt in the Arabian–Caucasus collision region. The magmatic sources were located at depths of 35–40 km, but had different compositions depending on the nature of the rocks in this transverse highly thermal zone. Volcanic products are basaltic material in the Arabian plate, where the Earth's crust thickness does not exceed 30–35 km. In Armenia, where the buried Mesozoic oceanic crust could be remelted, they are calc-alkaline, mostly andesitic, and in the Great Caucasus, where Earth's crust is thicker (45–50 km), they are dacitic. The large late Quaternary stratovolcanoes like the Elbrus, Ararat and Nemrut, do not show any control by crustal active structures. But small centres of areal volcanism are concentrated in structures of local relative extension within the compressed collision belt. We found three types of such extension structures. In the Druz plateau (1 in Fig. 7) the small volcanoes are located along the

Fig. 7. Map of active faults and the Late Pleistocene and Holocene volcanic rocks (dotted) in the region of the Arabian–Eurasian collision, compiled by V.G. Trifonov and A.S. Karakhanian.

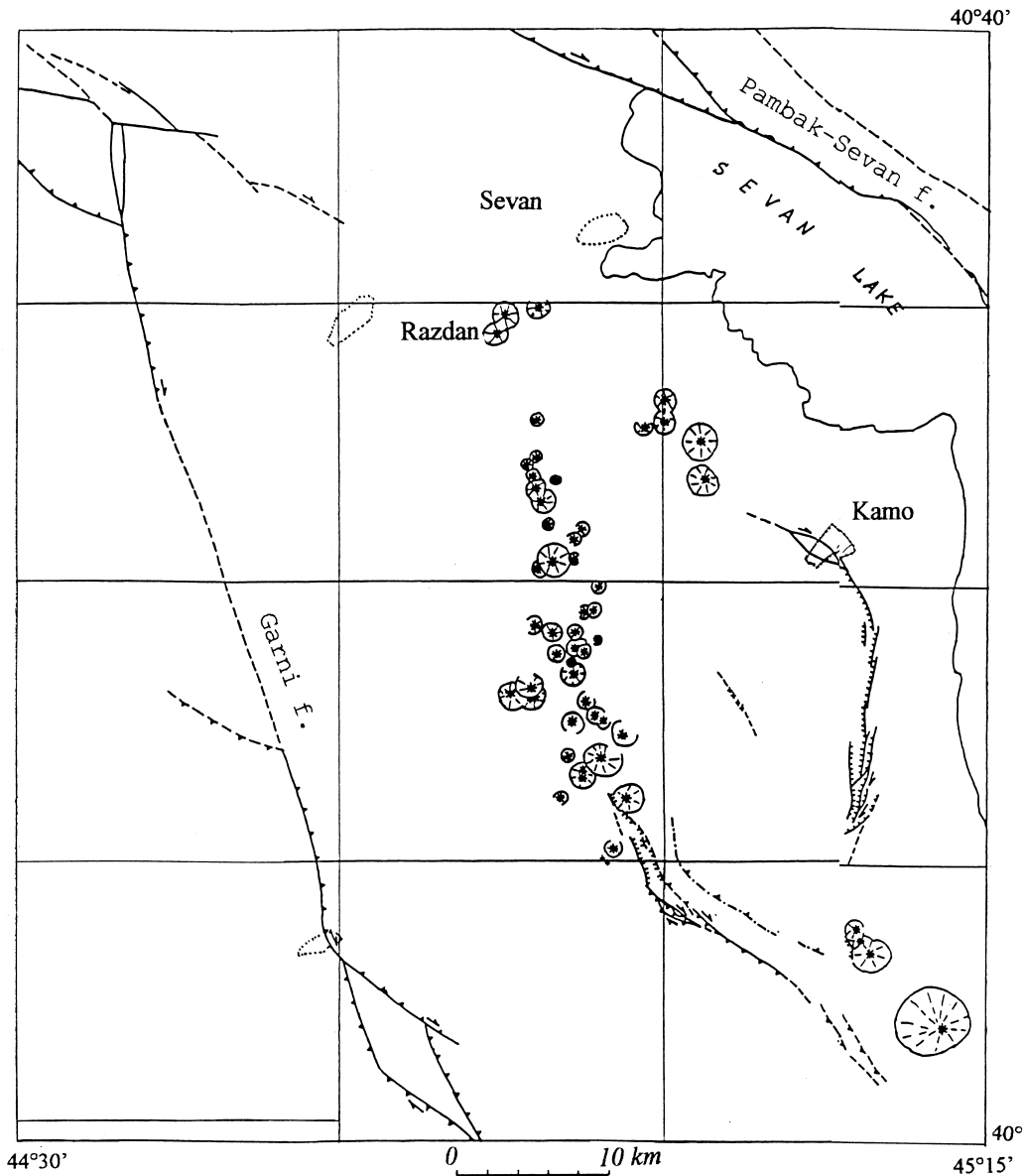


Fig. 8. Map of active faults and Late Pleistocene volcanoes in the Gegham Upland, Armenia, compiled by A.S. Karakhanian and V.G. Trifonov. The symbols for active faults are explained in Fig. 7.

normal and extension faults associated with the Levant sinistral fault zone. In Armenia (2 and 3 in Fig. 7) the volcanoes use the extension and oblique (normal-dextral) faults within pull apart basins in strike-slip zones. These are the Syunik basin in the Pambak–Sevan–Khanarassar dextral fault zone (Karakhanian et al., 1997) and the large Gegham structure between

the Pambak–Sevan–Khanarassar and Garni dextral fault zones (Fig. 8). The north-trending volcanic chains of the Djavakhet upland (4 in Fig. 7) are located in front of the North Armenian arc of active faults, and an extension of the area is produced by the northern drift and pressure of the Lesser Caucasus. It is interesting that volcanoes like the Ararat

are characterized by differentiated products of eruptions, while the small centres of areal volcanism produce undifferentiated material. Probably, structural control facilitates the magma penetration into the land surface and does not create conditions for its differentiation.

The axes of principal shortening C_3 in the field of tensors of seismotectonic deformation strike mostly north–south, i.e. they are oriented in general similarly to the M_3 axes of the tectonic deformation. However, there are essential differences in orientation between the eastern flank of Qaidam, the eastern Tien Shan, the eastern Sayans, the southern Caspian Sea and the central Black Sea regions. The directions of the principal lengthening C_1 and intermediate C_2 axes of the seismotectonic deformation are more variable than the M_1 and M_2 axes of the tectonic deformation. These differences can be explained partly by inaccuracy of the data and partly by the short period of instrumental seismicity (some earthquakes are related to secondary small faults that have not been identified, or are taken into account in our calculation of tectonic deformation). But there is a principal difference: earthquake rupture is often characterized by a bigger vertical component of motion and by a corresponding deviation of the principal axes of deformation relative to the tectonic motion and deformation in the same fault zones. The additional vertical component can be contributed by some local sources of the stress field, such as crustal irregularities and chemical transformations in rocks (Ivanova and Trifonov, 1998).

Acknowledgements

The studies were supported by the International Science Foundation (Grant MPJ000) and the Russian State Scientific Program ‘Global Changes of Environment and Climate’ (Project 1.1.4).

References

- Ioffe, A.I., Kozhurin, A.I., 1996. Database of active faults of Eurasia. *J. Earthquake Prediction Res.* 5, 431–435.
- Ioffe, A., Govorova, N., Volchkova, G., Trifonov, R., 1993. Data base of active faults for the USSR area. *Geoinformatics* 4, 289–290.
- Ivanova, T.P., Trifonov, V.G., 1998. Seismogenerating properties of the upper crust (in Russian). Proc. 31st All-Russian Tectonic Conf. Tectonics and Geodynamics: General and Regional Aspects, I, GIN RAS Publ., Moscow, pp. 219–222.
- Jaeger, A., Cook, G., 1969. *Fundamentals of Rock Mechanics*. Sci. Paperbacks, New York.
- Karakhanian, A.S., Trifonov, V.G., Azizbekian, O.G., Hondkarian, D.G., 1997. Relationship of Late Quaternary tectonics and volcanism in the Khanarassar active fault zone, the Armenian Upland. *Terra Nova* 9, 131–134.
- Kostrov, B.V., 1975. *The Mechanics of the Tectonic Earthquake Source* (in Russian). Nauka Press, Moscow.
- Riznichenko, Yu.V., 1977. Calculation of deformation of seismic flow of rocks (in Russian). *Izv. Akad. Nauk SSSR, Phiz. Zeml.* 10, 34–47.
- Sidorenko, A.V. (Ed.), 1978. *The Map of Faults in the USSR Territory and Adjacent Areas* (in Russian). Nedra Press, Moscow.
- Soboleva, O.V., 1988. Deformation of the Earth’s Crust of Tadzhikistan by Data on Focal Mechanisms of Earthquakes (in Russian). Dr. Sci. Thesis, Institute of Physics of the Earth, Moscow, 290 pp.
- Trifonov, V.G., 1985. Development of active faults. *Geotectonics* 19, 95–103.
- Trifonov, V.G., 1996. The map of active faults in Eurasia: principles, methods, and results. *J. Earthquake Prediction Res.* 5, 326–347.
- Trifonov, V.G., 1997. World map of active faults, their seismic and environmental effects. In: Giardini, D., Balassanian, S. (Eds.), *Historical and Prehistorical Earthquakes in the Caucasus*. Kluwer, Dordrecht, pp. 169–179.
- Trifonov, V.G., Machette, M.N., 1993. The world map of major active faults project. *Ann. Geofis.* 36, 225–236.
- Trifonov, V.G., Vostrikov, G.A., Trifonov, R.V., Soboleva, O.V., 1997. Recent Upper crust geodynamics of Central Asia. In: Giardini, D., Balassanian, S. (Eds.), *Historical and Prehistorical Earthquakes in the Caucasus*. Kluwer, Dordrecht, pp. 109–120.